

The AGB stars of the intermediate-age LMC cluster NGC 1846

Variability and age determination

T. Lebzelter¹ and P.R. Wood²

¹ Institute of Astronomy, University of Vienna, Tuerkenschanzstrasse 17, A1180 Vienna, Austria

² Research School for Astronomy & Astrophysics, Australian National University, Weston Creek, ACT 2611, Australia

Received / Accepted

ABSTRACT

Aims. To investigate variability and to model the pulsational behaviour of AGB variables in the intermediate-age LMC cluster NGC 1846.

Methods. Our own photometric monitoring has been combined with data from the MACHO archive to detect 22 variables among the cluster's AGB stars and to derive pulsation periods. According to the global parameters of the cluster we construct pulsation models taking into account the effect of the C/O ratio on the atmospheric structure. In particular, we have used opacities appropriate for both O-rich stars and carbon stars in the pulsation calculations.

Results. The observed P-L-diagram of NGC 1846 can be fitted using a mass of the AGB stars of about $1.8 M_{\odot}$. We show that the period of pulsation is increased when an AGB star turns into a carbon star. Using the mass on the AGB defined by the pulsational behaviour of our sample we derive a cluster age of 1.4×10^9 years. This is the first time the age of a cluster has been derived from the variability of its AGB stars. The carbon stars are shown to be a mixture of fundamental and first overtone radial pulsators.

Key words. stars: AGB and post-AGB - stars: variables - Globular clusters: NGC 1846

1. Introduction

The cluster NGC 1846 belongs to an intermediate age population in the Large Magellanic Cloud (LMC). In contrast to the Milky Way the LMC harbours many clusters with an age around 1 to 5 Gyr (e.g. Girardi et al. 1995). These clusters thus provide an interesting possibility to study the late stages of stellar evolution for stars around 1.5 to $2.5 M_{\odot}$, while the globular clusters belonging to the Milky Way trace the evolution of stars of only up to about $0.9 M_{\odot}$.

While there is a general agreement in the literature that NGC 1846 is indeed an intermediate age cluster, the published values on global parameters of this system show some scatter. Derived metallicities can be roughly divided into two groups, one around $[\text{Fe}/\text{H}]=-1.5$ (Dottori et al. 1983, Leonardi & Rose 2003) and one around $[\text{Fe}/\text{H}]=-0.7$ (Bessell et al. 1983, Bica et al. 1986, Olszewski et al. 1991, Beasley et al. 2002). Probably the first determination of the metallicity was done by Cohen (1982) giving a value in between the two discussed metallicity levels, namely $[\text{Fe}/\text{H}]=-1.1$. The most recent determination of the cluster's metallicity is given by Grocholski et al. (2006), who derive a value of $[\text{Fe}/\text{H}]=-0.49 \pm 0$ based on the Ca triplet strength of 17 individual cluster members measured with the VLT.

Age values for NGC 1846 scatter between less than 1 Gyr (Frantsman 1988) and 4.3 Gyr (Bica et al. 1986). Mackey & Broby Nielsen (2007) give cluster ages from 1.5 to 2.5×10^9 years based on a comparison of the colour magnitude diagram and theoretical isochrones. The range in age thereby results from the usage of two different sets of isochrones. These ages correspond to masses on the AGB of about 1.3 to $1.8 M_{\odot}$. Mackey & Broby Nielsen (2007) also report on the probable existence of two populations in NGC 1846 with similar metallicity but separated in age by about 300 Myr.

A reddening of $A_V=0.45$ mag has been determined by Goudfrooij et al. (2006). Grocholski et al. (2006) note that NGC 1846 is probably suffering from differential reddening without giving any detailed numbers. Keller & Wood (2006) give a somewhat lower reddening of $E(B - V)=0.08$, i.e. an A_V value of 0.25 mag.

The first studies of the stellar content of NGC 1846 were published by Hodge (1960) and Hesser et al. (1976). A number of luminous stars on the Asymptotic Giant Branch (AGB) were identified and published with finding charts by Lloyd-Evans (1980). Throughout this paper we will use the naming given in Lloyd-Evans' publication (LEXX) except for H39, which follows the numbering from Hodge (1960). Details on individual AGB stars have been published in a number of papers. Frogel et al. (1980, 1990) and Aaronson & Mould (1985) gave near infrared photometry and m_{bol} values for most of Lloyd-Evans' AGB stars and a few more cluster objects, unfortunately without any finding chart. Tanabé et al. (1998) searched this cluster for extreme infrared stars, i.e. stars with a high circumstellar absorption in the visual range, but found none.

No investigations on the variability of the AGB stars in NGC 1846 has been published up to now. However, as most AGB stars are pulsating (forming the group of long period variables or LPVs) it seemed very likely that some light variability would be found in these stars. In a previous paper (Lebzelter & Wood 2005) we showed that the variability analysis of LPVs in a single stellar population like the globular cluster 47 Tuc allows one to investigate various fundamental aspects of AGB stars like the evolution of the pulsation mode or mass loss. With NGC 1846 we have chosen an interesting alternative target since its AGB stars are more massive and include a number of carbon stars.

2. Observations and data reduction

For the detection of AGB variables in NGC 1846 and the determination of their pulsation period two data sets were used. We started a photometric monitoring program using ANDICAM at the 1.3m telescope on CTIO which belongs to the SMARTS consortium¹. The plan was to obtain images of the cluster in *V* and *I* at a rate of approximately twice a week. However, this plan was not feasible due to a strong pressure on the observing time at this instrument. Still we got a total of 63 epochs between JD 2453584 and JD 2454048 with a gap between JD 2453856 and JD 2453950.

We used the pipeline reduced *V* and *I* images provided by the SMARTS consortium. The detection of variables and the extraction of the light curves was done using the image subtraction tool ISIS 2.1 (Alard 2000). The resulting light curves were searched for periodicities using Period98 (Sperl 1998). A maximum of three periods was used to fit the light change.

It turned out that the data set obtained at CTIO was very valuable to detect periods below 100 days, but that it was too short for a reliable determination of the long periods occurring in some of the AGB stars of NGC 1846. To improve our period determination we thus decided to access the MACHO database as the cluster was covered by this survey. We used the coordinates of the variable AGB stars detected within our CTIO time series to extract the corresponding MACHO light curves. Two additional long period variables not apparent in the CTIO data were also found. The MACHO data consisted of about 250 epochs over the time span between JD 2449001 and JD 2451546, i.e. about 2500 days. The cluster was in the overlap region of two MACHO frames so that for part of the sample two series of measurements were available. Periods were determined in the same way as for the CTIO data. Data both from the blue and from the red pass band were analyzed separately and gave very similar results. Also, time series from the two different MACHO frames resulted in the same periods within a few percent. Due to the significant separation in time and due to the different filter systems no attempt was made to combine the MACHO and the CTIO data.

Periods determined from both data sets were then compared with each other. The agreement for periods shorter than about 100 days was quite good (differing by a maximum of 10 percent) taking into account the significant irregularities found on top of the regular light change. An average period was calculated from the two data sets and used in the further analysis. For LE16 and a previously unidentified variable, LW1, the MACHO light curve was not useable. For H39 no counterpart could be identified in the MACHO data base. All longer periods were taken from the MACHO data. Compatibility of the MACHO period with the data set from CTIO was checked by eye in all these cases.

The uncertainties of the periods, calculated with a least square fit approach, are less than a few percent. For the MACHO data set, photometric errors were taken from the MACHO database. Typical values are below 0^m.01. For the CTIO data set we estimate a typical error of 0^m.01.

As part of the CTIO time series we obtained near infrared time series in *J* and *K* using the same instrument. This data set covers roughly three months and allows us to estimate the light variability in the near infrared. Standard data reduction was applied to the near infrared images using IRAF. The background was subtracted using dithering. The *J* and *K* magnitudes were transformed to the 2MASS system using the transformation from

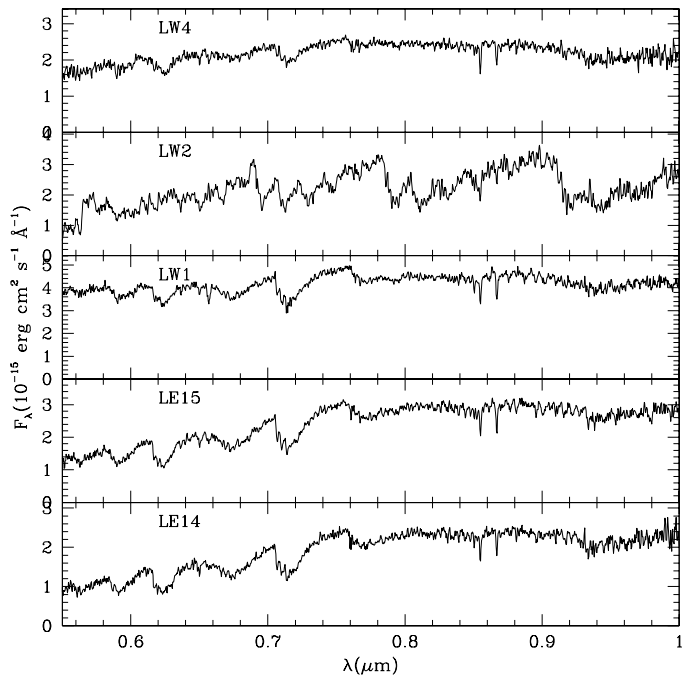


Fig. 1. Spectra of the NGC 1846 AGB variable stars without a previous spectral type.

Carpenter (2001). A set of reference stars within the cluster with near infrared photometry data from 2MASS was chosen to set the zero point for each epoch. These stars remained constant within $\pm 0^m.02$ relative to each other on all frames. This value can also be seen as the typical accuracy achieved for the variables.

Additional *J* and *K* photometry was obtained with the near-infrared array camera CASPIR (McGregor et al. 1994) on the 2.3m telescope of the Australian National University at Siding Spring Observatory. The *J* and *K* magnitudes on the CASPIR system were converted to the 2MASS system using the transformations in McGregor (1994) and Carpenter (2001). From these data we also obtained near infrared photometry for a large number of non variable, low luminosity AGB and RGB stars required for calibrating the models (see below).

For 5 variable stars with a previously unknown spectral type, spectra were obtained with the Dual Beam Spectrograph on the ANU 2.3m telescope at Siding Spring Observatory. The spectra are shown in Fig. 1 and the spectral types are listed in Table 2. For the O-rich stars, the spectral types were based on the strengths of the TiO bands at 616 nm and 705 nm. LW4 appears to be of late K spectral type while LW1, LE14 and LE15 are of early M spectral type. The C₂ bandhead at 564 nm and the strong CN bandheads at 692 and 788 nm clearly identify LW2 as a carbon star (see Turnshek et al. 1985 for an atlas of K, M, S and C star spectra).

3. Results

A total of 23 red variables were detected within the CTIO/ANDICAM field. Nineteen of these could be identified with AGB stars found by Lloyd-Evans (1980). For two of the stars, LE9 and LE18 variability was detected, but no period could be determined. Four further variables had no previous identifier in the literature. Their coordinates are given in Tab. 1. Similar to our approach in Lebzelter & Wood (2005), we named them with a prefix LW followed by a number.

¹ www.astronomy.ohio-state.edu/ANDICAM/

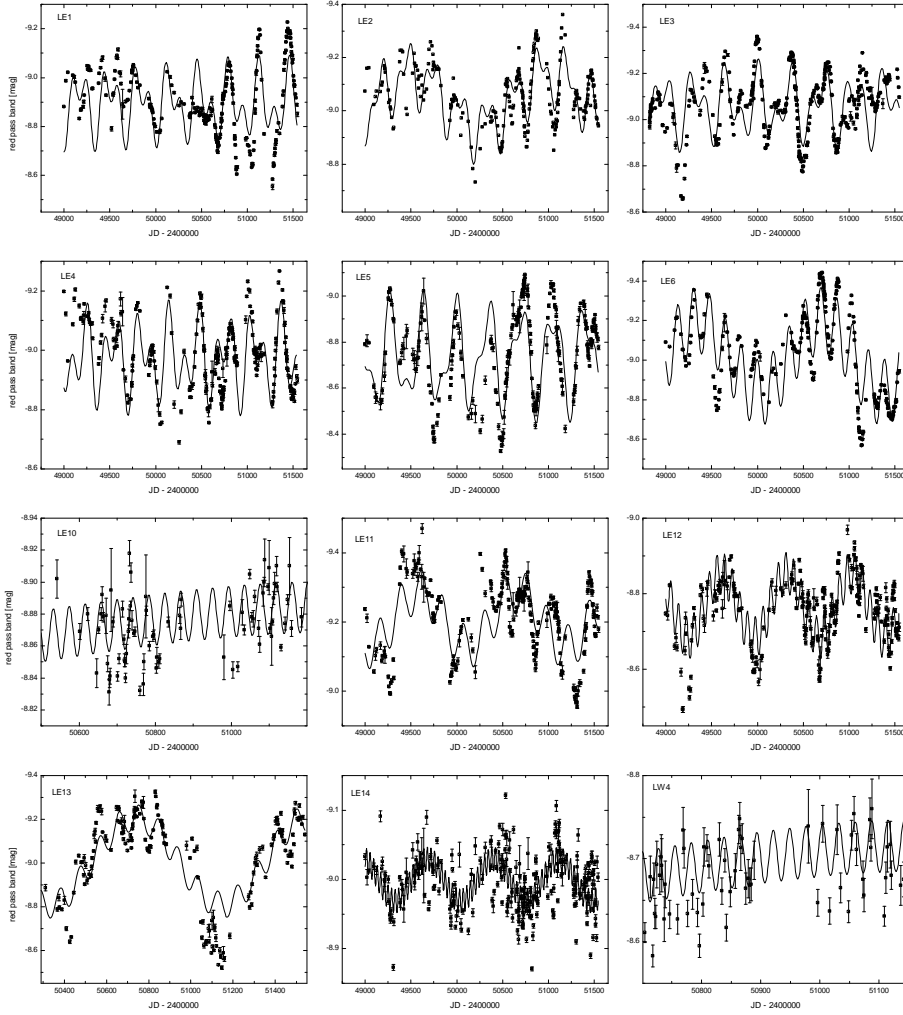


Fig. 2. MACHO light curves of the variables of our survey showing long periods. Fourier fits with up to two periods are shown. Note that the y-axis scale varies from star to star. For LE13 only part of the light curve is plotted for a better illustration of the short period light change.

Table 1. Coordinates from the 2MASS catalogue for variables with no identifier in the literature. For cross correlation with infrared sources identified by Tanabé et al. (2004a) see sect. 5).

Ident	RA (2000)	DE (2000)	comment
LW1	05:07:36.96	-67:27:56.9	
LW2	05:07:40.26	-67:27:40.3	
LW3	05:07:54.46	-67:24:46.2	prob. non-member
LW4	05:07:34.15	-67:27:48.5	

For stars with their light change dominated by long periods, MACHO light curves with corresponding Fourier fits are presented in Fig. 2. For the shorter period stars we show the CTIO data with the corresponding Fourier fits in Fig. 3. LW3, shown in Fig. 3, is obviously a nicely periodic (83 d), red ($(J - K)_{2MASS} = 1.17$) variable but, as it is located more than 3.5 arcmin away from the cluster center, we have to strongly doubt its membership to the cluster. This star will be excluded from the further analysis. Thus we have now a sample of 22 red variables associated with NGC 1846, 20 of them showing a periodic light change. The determined periods of these stars together with other basic data are listed in Tab. 2.

At a first glance two features of our sample are remarkable. First, multiperiodicity seems to be a common phenomenon among these stars. Only the weakest stars of our sample could be fitted with a single period. Thereby we observe two kinds of multiple periods, on the one hand two periods with a ratio of

about 2, and on the other hand long secondary periods, a well known feature of AGB variables in the Galactic field and in the MCs (e.g. Wood et al. 2004, Wood 2007). This long secondary period can be the dominant one as can be seen e.g. in LE12 and LE13 (see Fig. 2). Second, there are no large amplitude stars in NGC 1846, i.e. the classical miras seem to be missing. The light variations in the visual hardly exceed 1 mag. However, we find a considerable fraction of stars in the period range typically occupied by the miras (i.e. around 300 days).

Tanabé et al. (2004b) found a rapid increase in light amplitude once the star reaches the tip of the AGB. We see a similar relation between the light amplitude and mean K and $J - K$ values (Fig. 4).

The near infrared measurements show only a slight scatter typically of the order of the estimated error of the individual measurements. This is not surprising given the low light amplitudes found in the visual data. One star, LE 5, clearly exhibits a light change above the error level. Its light curve is shown in Fig. 5. The same behaviour of the light change as in the visual can be seen clearly. As the time series spans only a time interval of about 3 months long time changes are not properly covered. Thus we cannot exclude that the true light amplitude in the near infrared is larger than our estimate. The variation of about 0.2 mag seen for LE5 in J and about 0.15 mag in K correspond to about 0.4 mag in the visual light curve. As the light amplitude of our sample stars hardly exceeds 1 mag in the visual we can

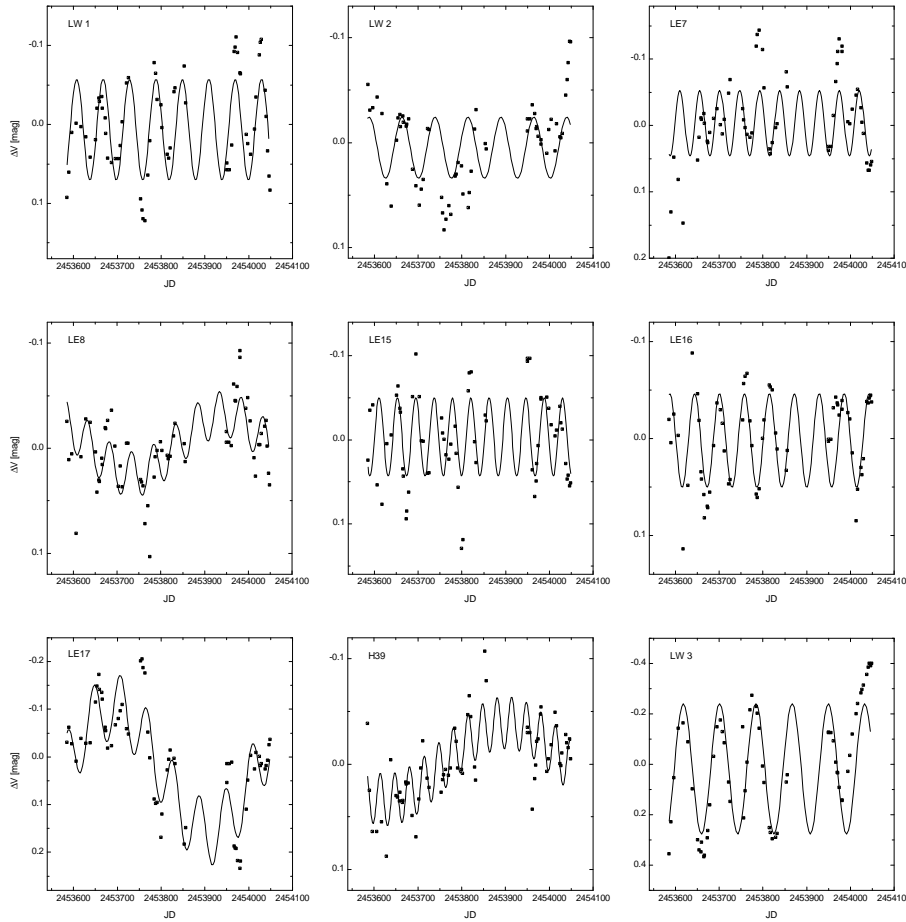


Fig. 3. ANDICAM/CTIO light curves of the variables of our survey dominated by short periods. Fourier fits with up to two periods are shown. Note that the y-axis scale varies from star to star. LW3 is probably not a member of NGC 1846 (see text).

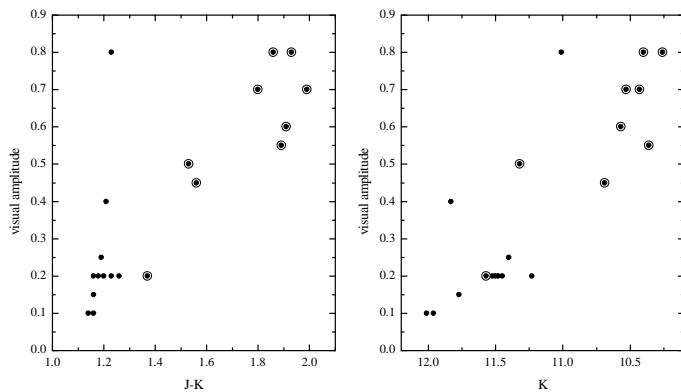


Fig. 4. Amplitude vs. K (right panel) and $J - K$ (left panel). No correction has been obtained for the difference in the filter pass-band between the MACHO and the ANDICAM time series. The amplitude given corresponds to the maximum light difference found in our time series. O-rich and C-rich stars are marked by dots and circled dots, respectively.

estimate that the total amplitude in J and K will be less than 0.6 and 0.4 mag, respectively.

Near infrared colour changes are also very small (see Fig. 5). We used our time series to calculate mean K and $J - K$ values for the further analysis. Our values are in reasonable agreement with the 2MASS data.

4. Pulsation models

Given the large number of LPVs now known in NGC 1846, we can now attempt to model the period-luminosity (PL) laws. For our models, we adopt the following parameters: distance modulus $(m - M)_V = 18.54$ and reddening $E(B - V) = 0.08$ (Keller & Wood 2006), helium mass fraction $Y = 0.27$ and a metal abundance $Z = 0.004$ (following Grocholski et al. 2006).

Below, we derive the mass of the AGB stars by fitting their period-luminosity (PL) relations, using the values mentioned above as a guide only. We note that the variables in this cluster are mostly of relatively small amplitude so that high mass loss rates are unlikely to have begun. It is also known that red giant mass loss prior to the superwind phase in intermediate mass stars with $M \sim 1.5 M_\odot$ is much less significant than in lower mass red giant stars such as those in globular clusters. We therefore assume a constant mass along the AGB where our variables are found.

The static and linear non-adiabatic pulsation models were created with updated versions of the pulsation codes described in Fox & Wood (1982). For temperatures above $\log T = 3.75$, the interior opacities of Iglesias & Rogers (1996) were used, including tables with the carbon enhancements required for carbon stars. For temperatures below $\log T = 3.75$, a scheme similar to that of Marigo (2002) was used for both oxygen-rich and carbon-rich opacities. Molecular contribution due to CN, CO and H_2O and a contribution due to metals of low ionization potential were added to low temperature opacities for zero-metallicity mixtures of Alexander & Ferguson (1994). Details will be given elsewhere. The core mass M_c was obtained from the $L - M_c$ relation of Wood & Zarro (1983).

Table 2. The AGB variables of NGC 1846. Reddening corrected photometry values are given. Periods are given in days. Multiple periods are listed in consecutive lines. A colon marks an uncertain period. Spectral types (last column) are from Frogel et al. (1990, see references therein) except for LE8 and LE13 which are taken from Lloyd-Evans (1983). LW3 is probably not a cluster member and thus not listed.

Ident	P	K	$J - K$	$\log L/L_{\odot}$	$\log T_{\text{eff}}$	Spec.
LE1	170	10.53	1.80	3.859	3.428	C
	325					
LE2	150	10.57	1.91	3.835	3.411	C
	289					
LE3	189	10.43	1.99	3.888	3.397	C
	351					
LE4	173	10.36	1.89	3.920	3.414	C
	307					
LE5	188	10.26	1.93	3.958	3.407	C
	355					
LE6	172	10.40	1.86	3.905	3.417	C
	1401					
LE7	47	11.40	1.19	3.670	3.565	M
	650					
LE8	51	11.23	1.23	3.719	3.557	S
	long					
LE10	41	11.96	1.16	3.463	3.571	K
LE11	227	10.69	1.56	3.842	3.470	C
	1066					
LE12	86	11.32	1.53	3.598	3.476	C
	716					
LE13	92	11.01	1.23	3.806	3.557	S
	837					
LE14	60	11.52	1.20	3.618	3.563	M
	715:					
LE15	41	11.48	1.26	3.607	3.553	M
	32:					
LE16	57	11.50	1.16	3.645	3.570	M
LE17	61	11.83	1.21	3.491	3.562	M
H39	33	11.77	1.16	3.538	3.571	M
LW1	60	11.45	1.18	3.655	3.567	M
LW2	75	11.57	1.37	3.545	3.506	C
LW4	27	12.01	1.14	3.448	3.573	K

Since we are computing pulsation periods, it is important to get the radii (and hence T_{eff}) of the models correct. In order to produce the correct T_{eff} on the AGB, the model AGB had to be made to coincide with the AGB of NGC 1846. The observational AGB was obtained by converting K and $J-K$ of the variables and non-variables in the cluster to M_K and $(J-K)_0$ using the distance modulus and reddening given above. Then, for O-rich stars, M_K and $(J-K)_0$ were converted to $\log L/L_{\odot}$ and $\log T_{\text{eff}}$ using the transforms in Houdashelt et al. (2000a; 2000b) (the 2MASS J and K values were first transformed to the SAAO system, similar to that of Houdashelt et al., using the transforms in Carpenter 2001). For C-rich stars, M_K and $(J-K)_0$ were converted to $\log L/L_{\odot}$ and $\log T_{\text{eff}}$ using the $((J-K)_0, T_{\text{eff}})$ relation from Bessell, Wood & Lloyd Evans (1983) and the bolometric correction to K from Wood, Bessell & Fox (1983). Figure 6 shows the NGC 1846 stars in the theoretical HR-diagram.

In order to match the models to the observed AGB, the mixing-length in the convection theory was set so that the O-rich, $Z=0.004$ models matched the T_{eff} of the O-rich stars in NGC 1846. As noted above, all our models have the same mass of $1.8M_{\odot}$: as explained below, this mass is required in order to get the correct pulsation periods. It was found that a constant mixing-length gave an AGB that decreased its T_{eff} too rapidly

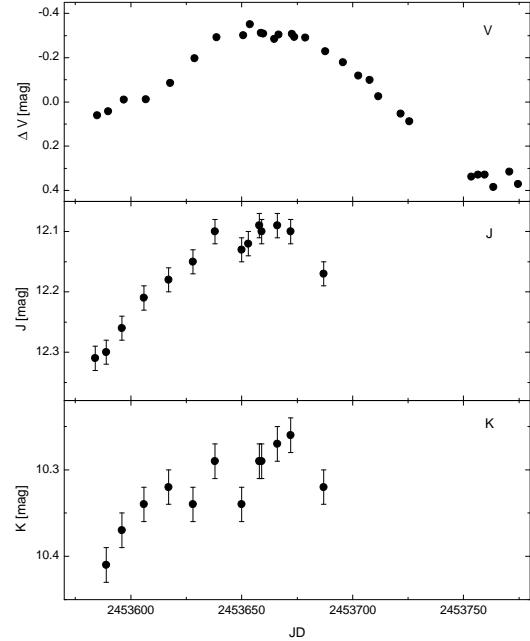


Fig. 5. Near infrared light variations of LE5 in J (middle panel) and K (lower panel) from CTIO/ANDICAM data. For comparison the visual light curve (CTIO/ANDICAM) for the same time span is shown (upper panel).

with increasing L (this is a general problem with all models e.g. the tracks or isochrones of Girardi et al. 2000). It was found that the ratio of mixing-length to pressure scale height α needed to increase slowly with L in order to obtain the correct slope for the theoretical giant branch (α was found to vary linearly with $L^{0.3}$). This can be seen in Table 3.

It is clear from Figure 6 that above about $\log L/L_{\odot} = 3.8$ ($L = 6310L_{\odot}$), all stars in NGC 1846 are C stars. For $L > 6000L_{\odot}$, we therefore assumed that C/O increased linearly with $\log L/L_{\odot}$: this corresponds to a constant rate of carbon dredge up since $\frac{d \log L}{dt}$ averaged over a shell flash cycle is constant for AGB stars (Wood 1974). We assumed that C/O reached 3 at $L = 9000L_{\odot}$, roughly the luminosity of the brightest AGB star in the cluster. We have no estimates of C/O for the stars in the cluster but values of C/O ~ 3 at the end of AGB evolution are indicated by planetary nebulae in the LMC (Stanghellini et al. 2005).

The model AGB created with the varying C/O ratio and C-rich opacities is shown in Figure 6. As soon as C/O passed through 1.0, T_{eff} decreased rapidly as the CN molecule and its opacity became more prominent. When C/O ~ 1.3 , essentially all the N atoms are bound to C atoms which are not bound up in CO. Thus the decrease in T_{eff} is not as rapid with further increases in C/O.

It is notable that the model T_{eff} values are not as cool as the T_{eff} values estimated for the observed stars by converting $J-K$ to T_{eff} . As shown below, the model T_{eff} values lead to quite a good match between observed and predicted pulsation periods, suggesting that the model T_{eff} values are reliable. This would indicate that the most luminous and cool C stars in NGC 1846 are warmer than estimated here. This could be because they have significant circumstellar shells leading to reddening of the stars, or because the conversion from $J-K$ to T_{eff} is incorrect.

The dashed line in Figure 6 is the track that would be followed by a C-rich star (with C/O = 2 in the case shown) undergoing a helium shell flash. During the He-burning part of the

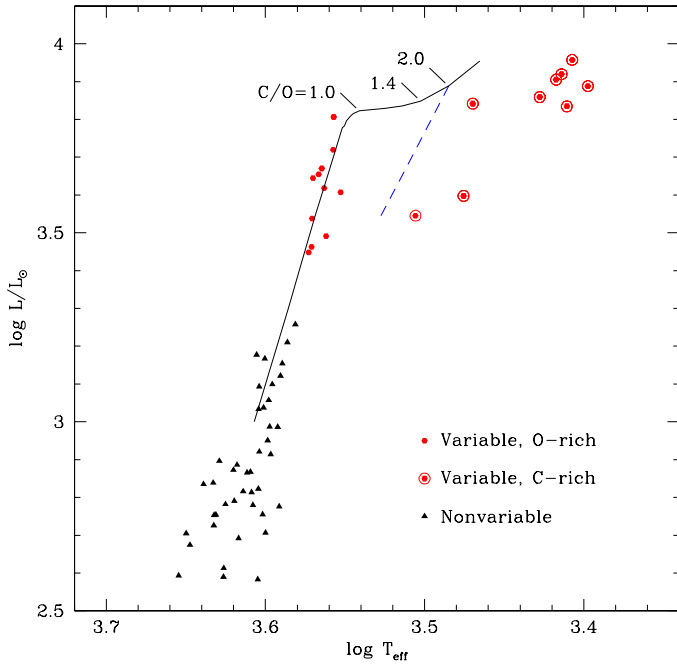


Fig. 6. The tip of the NGC 1846 giant branch in the HR-diagram. The variable and non-variable stars are shown along with their spectral types. The solid line is the theoretical giant branch, which has C/O increasing when L is greater than $6000 L_{\odot}$ (see text). Values of C/O are indicated at several points on the theoretical track. The dashed line is the line which a C-rich star will follow when its luminosity declines and rises during a helium shell flash cycle.

shell flash cycle, AGB stars of mass $1-2 M_{\odot}$ decline in luminosity by roughly a factor of 2 (Vassiliadis & Wood 1993) and spend a reasonable fraction of the cycle time near the low luminosity part of the cycle. We suggest that the two stars with $\log(L/L_{\odot}) < 3.7$ and $\log T_{\text{eff}} < 3.52$ are stars in this phase (both stars are C stars).

5. Discussion

Having matched the O-rich models to the observed values of T_{eff} , we ensure that the models matched the observed pulsation periods of the O-rich stars. If not, the mass was altered, and new calculations of the giant branch track and the pulsation periods were made. It was found that a mass of $1.8 M_{\odot}$ gave the best fit between observations and theory for the O-rich stars. This corresponds to a cluster age of 1.4×10^9 years using the isochrones of Girardi et al. (2000)². The fit is shown in Figure 7 and the model details are given in Table 3. It is clear that all the O-rich stars, with the exception of LE 17 near $\log P = 1.8$ and $\log L/L_{\odot} = 3.49$, are first or second overtone pulsators (the stars with long secondary periods are not considered here).

It is clear from the models that as the C/O ratio increases beyond 1.0, the periods of all modes increase rather rapidly due to the increase in radius and decrease in T_{eff} caused by the molecules in the C-rich atmospheres. Furthermore, it can be seen that the C stars fall quite nicely on two sequences corresponding to pulsation in the first overtone and fundamental modes. In

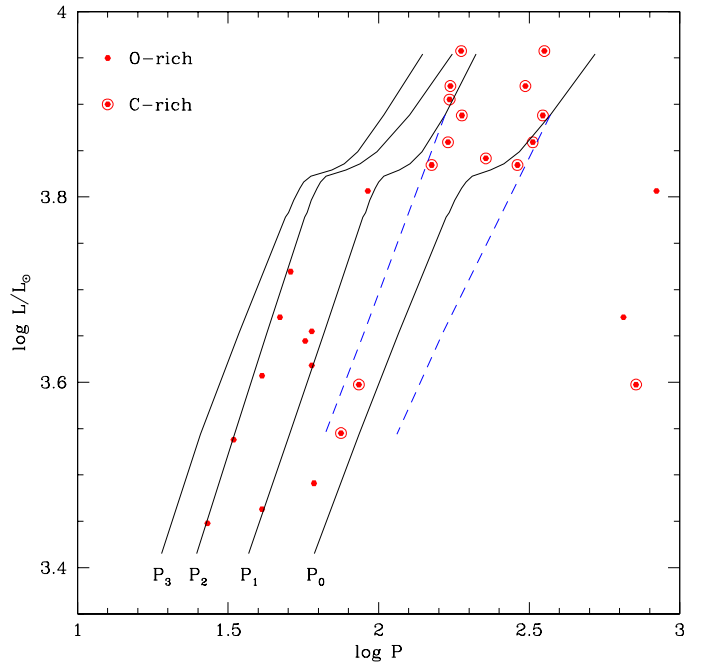


Fig. 7. The $\log(L/L_{\odot})$ - $\log P$ diagram for NGC 1846 stars and models. The fundamental mode and the first three overtones are shown for models with L near the H-burning maximum of the He shell flash cycle (solid lines). For AGB stars in the He-burning phase of the flash cycle, only the fundamental and first overtone modes are shown (dashed lines).

the absence of these C-rich models, it would have been natural to explain the C stars as fundamental mode pulsators scattering broadly around an extension of the fundamental mode O-rich sequence.

The fit of the models to the observed C star points is not perfect. This is not surprising given the rather elementary method used to compute the C-rich opacities, combined with the fact that we do not really know the C/O ratios in these stars. Furthermore, as mentioned above, the stars move up and down in luminosity during a He-shell flash cycle by factors of about 2 in luminosity (Vassiliadis & Wood 1993). The dashed lines in Figure 7 show how the fundamental and first overtone periods would vary over a shell flash cycle for a star with C/O = 2. It seems most likely that the two C stars with $\log L/L_{\odot} < 3.6$ are near the luminosity minimum of a shell flash cycle (where AGB stars spend about 20% of their time).

In general, the theoretical and observed periods for the C-stars agree reasonably well. This indicates that the radii and T_{eff} values of the models agree well with the real values for these stars and the assumption that the temperatures indicated by the near infrared colours are misleading.

It is somewhat strange that the most luminous of the C stars appear to have shorter pulsation periods than the less luminous C stars. One way for this to occur would be to decrease the C/O ratio in the most luminous C stars by hot-bottom burning. However, at $1.8 M_{\odot}$, the mass is too low for hot-bottom burning, since AGB masses greater than about $4 M_{\odot}$ are required for hot-bottom burning to be significant. Another explanation may be that the nonlinear pulsation period differs from the linear pulsation period when the pulsation amplitude increases, as noted in Lebzelter & Wood (2005). The visual light amplitudes give no indication for this as the amplitudes of the carbon stars are all very similar (see Fig. 4). In the infrared, as shown in Fig. 5,

² Using the BaSTI isochrones (Bedin et al. 2005) we find an age of 1.9×10^9 years for a $1.8 M_{\odot}$ star to reach the AGB (using the same parameters as Mackey & Broby Nielsen 2007).

Table 3. The pulsation models

L/L_{\odot}	M/M_{\odot}	M_c/M_{\odot}	ℓ/H_p	$\log T_{\text{eff}}$	C/O	P_0	P_1	P_2	P_3
AGB stars with L near the H-burning maximum of the flash cycle									
6000	1.8	0.596	1.882	3.5516	0.324	167.7	88.7	56.8	49.1
6069	1.8	0.597	1.884	3.5503	0.400	171.6	90.4	57.9	50.2
6256	1.8	0.601	1.890	3.5490	0.600	179.1	93.5	59.8	52.2
6448	1.8	0.604	1.895	3.5465	0.800	188.8	97.5	62.4	54.8
6547	1.8	0.605	1.897	3.5447	0.900	195.0	100.0	64.1	56.4
6647	1.8	0.607	1.900	3.5409	1.000	204.6	104.0	66.9	59.5
6748	1.8	0.609	1.903	3.5248	1.100	235.4	117.1	77.9	70.0
6851	1.8	0.611	1.905	3.5139	1.200	260.4	127.1	86.8	76.8
7062	1.8	0.614	1.911	3.5025	1.400	293.3	139.4	98.8	85.2
7734	1.8	0.626	1.927	3.4849	2.000	371.4	166.1	126.8	104.0
9000	1.8	0.647	1.955	3.4652	3.000	523.7	210.8	175.7	140.1
AGB stars in the He-burning phase of the flash cycle									
7734	1.8	0.626	1.927	3.4849	2.000	371.4	166.1	126.8	104.0
4500	1.8	0.626	1.836	3.5140	2.000	163.3	89.3	59.1	53.4
3500	1.8	0.626	1.800	3.5276	2.000	114.9	66.4	43.6	31.5

Notes: All models helium abundance $Y = 0.26$. The initial metal abundance (before third dredge-up) is $Z = 0.004$. ℓ/H_p is the ratio of mixing-length to pressure scale height. P_0 , P_1 , P_2 and P_3 are the linear nonadiabatic periods (in days) of the fundamental, 1st, 2nd and 3rd overtone modes.

the star with the largest amplitude in our data set is LE5 which is also the most luminous star of our sample. This may indeed indicate that the shorter periods at the tip of the AGB can be explained by nonlinear effects. However, as mentioned above, our near infrared time series are too short for a definite conclusion on this point.

A reduction in stellar mass due to significant amounts of mass loss can not explain the shorter periods of the most luminous C stars since this would *increase* the pulsation period. In general, we have not found it necessary to invoke any significant reduction in mass with luminosity up the AGB in these calculations. We note that this contrasts with the stars in 47 Tuc studied by Lebzelter & Wood (2005) where a significant amount of mass loss was found on the AGB. As noted briefly in Section 4, this is as expected. The stars being studied here and in 47 Tuc appear to have relatively low mass loss rates where a Reimers' mass loss law may apply. In such a case, the mass loss rate is proportional to LR/M . For a given L , this functional dependence suggests that the intermediate mass ($\sim 1.8 M_{\odot}$) stars in NGC 1846 will have lower mass loss rates than the low mass ($\sim 0.9 M_{\odot}$) 47 Tuc stars because of the higher mass. In addition, the giant branch temperature increases with stellar mass so the radius will be smaller at a given L in NGC 1846. The consequence of the expected lower mass loss rate in NGC 1846 is that a smaller amount of mass is lost on the giant branches up to a given L . The fractional change in mass in NGC 1846 is even smaller because of the higher mass.

An independent check of the mass loss can be obtained from mid-IR photometry looking for indications of an infrared excess due to dust emission. NGC 1846 was covered by the SAGE mid-IR survey (Meixner et al. 2006). Blum et al. (2006) find [8]-[24] as an indicator for mass loss. For five of the carbon stars in our sample (LE1, LE2, LE3, LE6 and LE11) the corresponding photometry can be found in the SAGE point source data base. All of them show an [8]-[24] colour typical for low mass loss stars. We recall that Tanabé et al. (1998, 2004a) did not find any dust enshrouded objects in this cluster. For two sources Tanabé et al. (2004a) list no identification from the literature. Their object 16 is obviously the variable LW2. Object 8, the weakest object in their list of mid infrared sources, corresponds to LW4.

Using the SAGE list of point sources we checked for bright objects at $24 \mu\text{m}$ with no or a very weak optical counterpart. Indeed we found three sources fulfilling this criterion, but their membership to the cluster is not very likely. In the appendix we give a more detailed description of these three sources. Thus we can derive from our findings that the AGB stars of NGC 1846 lose their mass in a quite short time at the end of the AGB phase.

The location of LE17 in the P-L-diagram remains somehow a mystery. While the two carbon stars found at $\log L/L_{\odot} = 3.57$ nicely agree with the expected location of a TP-AGB star close to its luminosity minimum, it is unlikely that this explanation also holds for LE17, which is the O-rich star slightly below in the P-L-diagram (Fig. 7). If it would be in the minimum of its TP cycle, it would be in a region exclusively occupied by C-rich stars during its maximum. A possibility may be that the star is located at the "knee" of the fundamental mode sequence at its maximum. Alternatively, the derived temperature and luminosity of this star may be wrong due to higher reddening of this object. Circumstellar reddening probably plays only a minor effect as there is no clear indication for this from mid-IR photometry (SAGE; Tanabé et al. 2004a). We further note that the star nicely fits onto the giant branch of NGC 1846 (Fig. 6), thus there is no indication for a significant reddening. For the same reason we may safely assume that the star is indeed a member of the cluster. Further investigations are required to understand the behaviour of this star.

6. Summary

Twenty two long period variable stars have been detected in the LMC cluster NGC 1846. Most of them were previously known AGB stars in this cluster. We have modelled the pulsation of O-rich and C-rich AGB stars in NGC 1846, taking into account the effects of the C/O ratio on the stellar structure. The stars fit nicely on several parallel $\log P$ - $\log L$ -relations. Similar to 47 Tuc (Lebzelter & Wood 2005), the LPVs populate the first and second overtone sequence at lower luminosities, while the more luminous stars are found on the first overtone and fundamental sequence. In addition to the separation by luminosity, there is also a difference related to the atmospheric chemistry. The O-

rich AGB variables are found to be first and second overtone pulsators. We show for the first time that the period of pulsation is increased when an AGB star turns into a carbon star because of the expansion of the star and the lowering of T_{eff} . The carbon stars are shown to fall on two sequences in the P-L-diagram, corresponding to pulsation in the fundamental and first overtone modes. Oxygen rich models would give a very poor fit to the PL relation for C stars and would predict fundamental mode pulsation only. We find that there has been no significant mass reduction from mass loss right to the tip of the observed AGB in NGC 1846. This is in agreement with mid-IR data. The mass of the AGB stars is $\sim 1.8 M_{\odot}$, corresponding to a cluster age of 1.4×10^9 years. This is the first determination of the age of a cluster based on the pulsational properties of its AGB variables and in excellent agreement with the value derived by Mackey & Broby Nielsen (2007) from isochrone fitting. However, the separation of the two populations found by the latter authors is too small to be detectable in the pulsational behaviour of the AGB stars.

Acknowledgements. TL has been funded by the Austrian FWF under project P18171-N02. PRW has been partially supported in this work by the Australian Research Council's Discovery Projects funding scheme (project number DP0663447). This paper utilizes public domain data obtained by the MACHO Project, jointly funded by the US Department of Energy through the University of California, Lawrence Livermore National Laboratory under contract No. W-7405-Eng-48, by the National Science Foundation through the Center for Particle Astrophysics of the University of California under cooperative agreement AST-8809616, and by the Mount Stromlo and Siding Spring Observatory, part of the Australian National University. This research is partly based on data obtained with the 1.3m telescope at CTIO, National Optical Astronomy Observatories, which is operated by the SMARTS consortium.

References

- Aaronson, M., Mould, J. 1985, ApJ, 288, 551
 Alard, C. 2000, A&A Suppl., 144, 363
 Alexander, D.R., Ferguson, J.W. 1994, ApJ, 437, 879
 Beasley, M.A., Hoyle, F., Sharples, R.M. 2002, MNRAS, 336, 168
 Bedin, L.R., Cassisi, S., Castelli, F., et al. 2005, MNRAS, 357, 1038
 Bessell, M.S., Wood, P.R., Lloyd-Evans, T. 1983, MNRAS, 202, 59
 Bica, E., Dottori, H., Pastoriza, M. 1986, A&A, 156, 261
 Blum, R.D., Mould, J.R., Olsen, K.A., et al. 2006, AJ, 132, 2034
 Carpenter, J.M. 2001, AJ, 121, 2851
 Cohen, J.G. 1982, ApJ, 258, 143
 Dottori, H., Pastoriza, M., Bica, E. 1983, Ap&SS, 91, 790
 Fox, M.W., Wood, P.R. 1982, ApJ, 259, 189
 Frantsman, J.L. 1988, Ap&SS, 145, 251
 Frogel, J.A., Persson, S.E., Cohen, J.G. 1980, ApJ, 239, 495
 Frogel, J.A., Mould, J., Blanco, V.M. 1990, ApJ, 352, 96
 Girardi, L., Chiosi, C., Bertelli, G., Bressan, A. 1995, A&A, 298, 87
 Girardi, L., Bressan, A., Bertelli, G., Chiosi, C. 2000, A&AS, 141, 371
 Goudfrooij, P., Gilmore, D., Kissler-Patig, M., Maraston, C. 2006, MNRAS, 369, 697
 Grocholski, A.J., Cole, A.A., Sarajedini, A., et al. 2006, AJ, 132, 1630
 Hesser, J.E., Hartwick, D.A., Ugarte, P. 1976, ApJS, 32, 283
 Hodge, P.W. 1960, ApJ, 132, 341
 Houdashelt, M.L., Bell, R.A., Sweigart, A.V. 2000a, AJ, 119, 1448
 Houdashelt, M.L., Bell, R.A., Sweigart, A.V., Wing, R.F. 2000b, AJ, 119, 1424
 Iglesias, C.A., Rogers, F.J. 1996, ApJ, 464, 943
 Keller, S.C., Wood, P.R. 2006, ApJ, 642, 834
 Lebzelter, T., Wood, P.R. 2005, A&A, 441, 1117
 Leonardi, A.J., Rose, J.A. 2003, AJ, 126, 1811
 Lloyd-Evans, T. 1980, MNRAS, 193, 87
 Lloyd-Evans, T. 1983, MNRAS, 204, 985
 Mackey, A.D., Broby Nielsen P. 2007, MNRAS, 379, 151
 Marigo, P. 2002, A&A, 387, 507
 McGregor, P.J., 1994, PASP, 106, 508
 McGregor, P., Hart, J., Hoadley, D., Bloxham, G. 1994, in: Infrared Astronomy with Arrays, ed. I. McLean (Kluwer), p.299
 Meixner, M., Gordon, K.D., Indebetouw, R., et al. 2006, AJ, 132, 2268
 Olszewski, E.W., Schommer, R.A., Suntzeff, N., Harris, H.C. 1991, AJ, 101, 515
 Sperl, M. 1998, Comm. Asteroseism., 111, 1

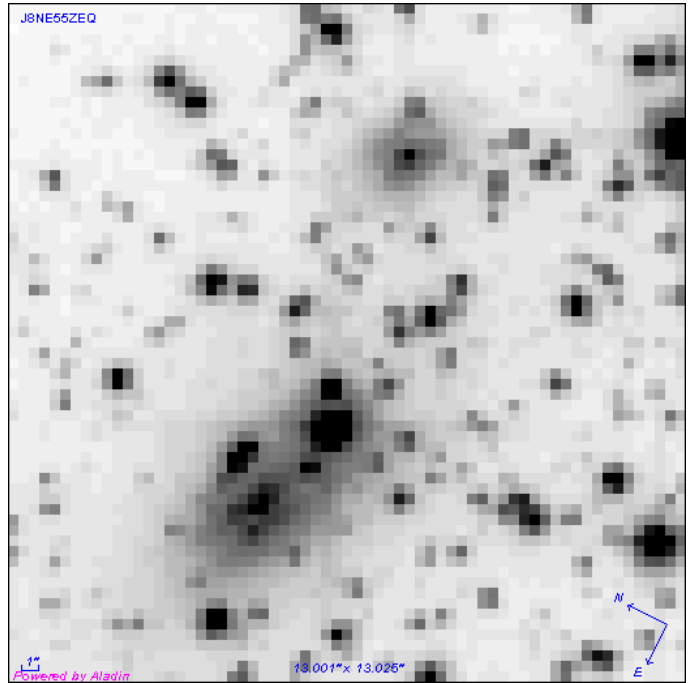


Fig. A.1. HST/ACS image showing source 1 (upper center) and 2 (lower center), respectively. The size of the image is approximately 13 x 13 arcsecs.

- Stanghellini, L., Shaw, R.A., Gilmore, D. 2005, ApJ, 622, 294
 Tanabé, T., Nishida, S., Nakada, Y., et al. 1997, Ap&SS, 255, 407
 Tanabé, T., Kucinskas, A., Nakada, Y., Onaka, T., Sauvage, M. 2004, ApJS, 155, 401
 Tanabé, T., Ita, Y., Matsunaga, N., et al. 2004, ASP Conf. Ser., 310, 295
 Turnshek, D.E., Turnshek, D.A., Craine, E.R. Boeshaar, P.C. 1985, An Atlas of Digital Spectra of Cool Stars (Western Research Company)
 Vassiliadis, E., Wood, P.R. 1993, ApJ, 413, 641
 Wood, P.R. 1974, ApJ, 190, 609
 Wood, P.R. 2007, ASP Conf. Ser. 362, 234
 Wood, P.R., Bessell, M.S., Fox, M.W. 1983, ApJ, 272, 99
 Wood, P.R., Zarro, D.M. 1981, ApJ, 247, 247
 Wood, P.R., Olivier, A.E., Kawaler, S.D. 2004, ApJ, 604, 800

Appendix A: 3 very red sources in the field of NGC 1846

The SAGE images show three sources in the area of NGC 1846 that are very prominent at $24 \mu\text{m}$ and have no clear counterpart in the visual. Table A.1 gives coordinates and flux values for the three objects.

All three sources are extended as can be seen on the F814W band HST/ACS images available in the HST data archive (program ID: 9891, PI: Gerard Gilmore) and shown in Figs. A.1 and A.2, respectively. Source 1 and 2 are located much closer to the cluster center than source 3. The location relative to the cluster is also visible from Fig. 1 of Mackey & Broby Nielsen (2007, where source 3 is located in the right part of the image just above the gap and source 2 on the upper left part. None of the three sources could be identified with any object in the list of Tanabé et al. (1998, 2004a).

Source 1 has no detectable counterpart at $2.2 \mu\text{m}$ but probably at 3.6 , 4.5 and $8 \mu\text{m}$. The energy distribution is plotted in Fig. A.3. The object is of rather circular shape with an approximate diameter of 2 arcseconds.

Source 2 looks elongated and is a little bit difficult to separate from a nearby star, probably a RGB star of NGC 1846 according

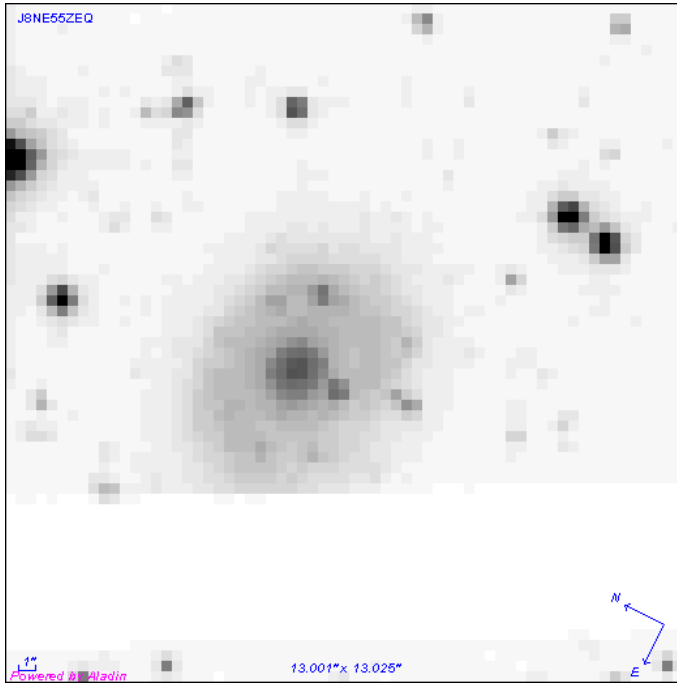


Fig. A.2. HST/ACS image of source 3 (in the middle above the gap). The size of the image is approximately 13 x 13 arcsecs.

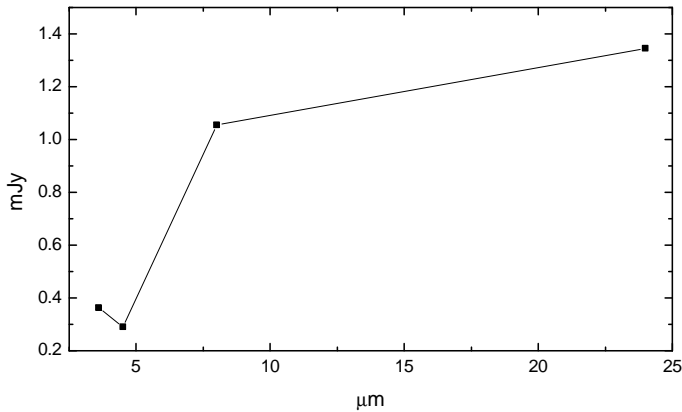


Fig. A.3. Mid-IR energy distribution of source 1 from SAGE data.

to its 2MASS J and K values. It is below the SAGE detection limit at $3.6 \mu\text{m}$, $4.5 \mu\text{m}$ and $5.8 \mu\text{m}$, respectively. A source is detected at $8 \mu\text{m}$ at a flux level of 0.585 mJy . The object has a size of about 3 to 4 arc seconds.

Source 3 is of slightly elongated shape with an approximate diameter of 5 arc seconds. The image reveals a central concentration and a few spots possibly related to this source. The central source is not present in the 2MASS point source catalogue and is also not visible on the 2MASS K frame. This object is most likely a background galaxy. Interpretation of sources 1 and 2 is more difficult. We suspect that due to their sizes and redness both are background galaxies. They seem to be far too weak at wavelengths shortward of $20 \mu\text{m}$ to represent dust enshrouded objects within the cluster.

Table A.1. Infrared sources in the field of NGC 1846. Coordinates and fluxes are taken from the SAGE catalogue.

Ident	RA (2000)	DE (2000)	$F_{24\mu}$ (mJy)
Source 1	05:07:33.21	-67:27:06.2	1.346
Source 2	05:07:34.42	-67:27:07.2	0.799
Source 3	05:07:34.94	-67:29:01.8	0.875